ELSEVIER

Catalysis Today 76 (2002) 149–159

CATALYSIS TODAY

www.elsevier.com/locate/cattod

Radiation absorption and rate constants for carbaryl photocatalytic degradation in a solar collector

Camilo A. Arancibia-Bulnes [a,*], Erick R. Bandala [b,1], Claudio A. Estrada [a]

[a] *Centro de Investigación en Energía, Universidad Nacional Autónoma de México, Apdo. Postal 34 Temixco, Morelos 62580, Mexico*
[b] *Instituto Mexicano de Tecnología del Agua, Paseo Cuahunáhuac 8532, Jiutepec, Morelos 62550, Mexico*

Abstract

We discuss an analytical model for the evaluation of radiation absorption in a tubular photocatalytic reactor. The model has no adjustable parameters and takes into account scattering in all directions. We compare the results of this model with those of Monte Carlo (MC) simulations and of a Lambert–Beer (LB) approximation, for a reactor illuminated by a parabolic solar concentrator. A good correspondence is found with the MC simulations. In particular, the model displays the correct saturation behavior of absorption for large catalyst particle concentrations, which is not obtained with the LB approximation. We have carried out experiments for the degradation of carbaryl in a solar parabolic collector (PC). The model is used to calculate the rate constant for this degradation from the experimental data. The theoretical model predictions reproduce well, the trends observed in the experiments.

Keywords: Photocatalysis; Radiation absorption; Solar collectors; Titanium dioxide; Carbaryl

1. Introduction

Photocatalytic degradation of pollutants by using solar energy is a very attractive technology for the remediation of contaminated water [1–3]. In some variants of this process solar ultraviolet (UV) radiation is absorbed by semiconductor catalyst particles suspended in water. In particular, TiO_2 photocatalytic particles are the most widely used for these applications.

The mathematical modeling required for the study and design of solar photocatalytic reactors includes radiation transport [4–6]. This is a complicated task due to the large amount of radiation scattering produced by the catalyst particles. In principle, these calculations can be done through the solution to the radiative transfer equation (RTE) which takes into account the effects of absorption and scattering of radiation. This can been done using numerical methods, like the discrete ordinates method [6–8] and Monte Carlo (MC) simulations [9,10]. However, both of these methodologies require large amounts of computer calculations and do not provide analytical formulas. From a practical point of view it is desirable to have simpler methods, which allow one to carry out approximate calculations with an acceptable degree of error.

In this work we present calculations for radiation absorption in a cylindrical photocatalytic reactor illuminated by a parabolic solar concentrator. For these purposes we use the P1 approximation to the RTE

Abbreviations: LB, Lambert–Beer; LVREA, local volumetric rate of energy absorption; MC, Monte Carlo; PC, solar parabolic collector; P1, P1 approximation; RTE, radiative transfer equation; UV, ultraviolet

* Corresponding author. Fax: +52-55-562-297-91.
E-mail address: caab@cie.unam.mx (C.A. Arancibia-Bulnes).
[1] Tel./fax: +52-777-319-4281.

0920-5861/02/$ – see front matter © 2002 Elsevier Science B.V. All rights reserved.
PII: S0920-5861(02)00215-8

Nomenclature

B_α	proportionality factor (m)
c	reactant concentration (g/l)
c_{light}	speed of light in vacuum
c_{L}	local reactant concentration (g/l)
c_{p}	catalyst concentration (g/l)
c_0	initial reactant concentration (g/l)
C_{g}	geometrical concentration of solar collector (dimensionless)
D	integration constant for local radiation ($\text{W m}^{-2}\,\text{nm}^{-1}$)
e_{L}	local volumetric rate of energy absorption ($\text{einstein m}^{-3}\,\text{s}^{-1}$)
f	probability density distribution for photon collision (m^{-1})
f_λ	spectral distribution of UV solar radiation (nm^{-1})
$F_{1\lambda}$	fraction of absorbed radiation (dimensionless)
$F_{1\lambda}^{\text{LB}}$	fraction of absorbed radiation in Lambert–Beer approximation (dimensionless)
$F_{1\lambda}^{\max}$	maximum fraction of absorbed radiation (dimensionless)
g	asymmetry parameter (dimensionless)
G	spectral local radiation ($\text{W m}^{-2}\,\text{nm}^{-1}$)
h	Planck's constant
I_λ	spectral specific intensity ($\text{W m}^{-2}\,\text{nm}^{-1}\,\text{sr}^{-1}$)
I_0^{B}	modified Bessel function of order 0 (dimensionless)
I_1^{B}	modified Bessel function of order 1 (dimensionless)
k	rate constant ($(\text{einstein m}^{-3})^{-\alpha}\,\text{s}^{\alpha-1}$)
K_{d}	transport (diffusion) constant (m^{-1})
l	reactor length (m)
$\hat{\mathbf{n}}_{\text{b}}$	unit vector normal to the tube boundary (dimensionless)
N_{a}	Avogadro's number
p	scattering phase function (dimensionless)
P_{abs}	total spectral power absorbed in the reactor (W nm^{-1})
P_{ent}	total spectral power entering the reactor (W nm^{-1})
p_{ext}	probability for photon collision
$\mathbf{q}$	radiative flux vector ($\text{W m}^{-2}\,\text{nm}^{-1}$)
q_{ent}	radiation flux entering the reactor ($\text{W m}^{-2}\,\text{nm}^{-1}$)
r	radial coordinate inside the reactor (m)
$\mathbf{r}$	vector coordinate inside the reactor (m)
$\mathbf{r}_{\text{b}}$	position vector for points on the tube boundary (m)
r_0	tube radius (m)
R_{m}	reactant mass transfer rate (mol s^{-1})
s	distance along propagation direction (m)
$\hat{\mathbf{s}}$	unit vector in the propagation direction (dimensionless)
t	time (s)
V_{R}	reactor volume (m^3)
V_{T}	system volume (m^3)
W	incoming beam solar UV radiation (W m^{-2})
z	linear coordinate along the tube (m)

Greek letters

α	exponent (dimensionless)
β_λ	extinction coefficient (m^{-1})
β_λ^*	mass extinction coefficient ($\text{m}^2\,\text{g}^{-1}$)
η_{eff}	optical collector efficiency (dimensionless)
θ	angular coordinate around the tube (rad)
κ_λ	absorption coefficient (m^{-1})
κ_λ^*	mass absorption coefficient ($\text{m}^2\,\text{g}^{-1}$)
λ	wavelength (nm)
ρ	reflectance of glass tube (dimensionless)
σ_λ	scattering coefficient (m^{-1})
σ_λ^*	mass scattering coefficient ($\text{m}^2\,\text{g}^{-1}$)
τ_λ	transmittance of glass tube (dimensionless)
ω	scattering albedo (dimensionless)
Ω	solid angle (sr)

[11, Chapter 9; 12, Chapter 14]. The proposed model is simple enough to allow for an analytical solution, with still enough complexity to take into account scattering of radiation in all directions. In addition, it does not contain any adjustable parameter. The results obtained with this model are compared directly with the more exact numerical MC simulations. The objective of this is to explore the applicability of this simplified model of radiation transport to photocatalysis.

The theoretical model is employed to carry out calculations of rate constants for the degradation of carbaryl in a solar parabolic collector (PC). Carbaryl, (1-naphthyl-*N*-methylcarbamate) is a carbamic type pesticide widely used in Mexico. Despite its moderate persistence, this xenobiotic has been detected in a wide number of sites from USA to Canada [13]. Moreover, this compound is degraded rather slowly by microorganisms. Previous studies have shown that it is possible to degrade carbaryl by using photocatalytic methodologies [14–16]. Nevertheless, these studies have been carried out only in the laboratory scale using simulated sun radiation [16].

2. Theoretical model

Using chemical actinometry, the amount of UV solar energy entering a photocatalytic reactor can be evaluated with a high precision. However, not all of this radiation is absorbed by the catalyst particles, and therefore useful for the degradation process. It is not a simple matter to determine the fraction of absorbed radiation from the entering radiation. Light scattering effects due to the rather small particles involved must be taken into account to avoid large errors [17]. It is difficult to deal with these effects mathematically, not to mention that values for the relevant physical parameters are not always available. Due to this, some times a simple expression of the kind of Lambert–Beer (LB) law is assumed (see for example [18]). In some cases, it is even considered that all available radiation is absorbed by the suspension. Both of these assumptions are very crude approximations.

A detailed knowledge of the distribution of the radiation field (and of absorbed energy) in a scattering medium can be obtained from a solution to the RTE [12].

$$\frac{\mathrm{d}I_\lambda(\mathbf{r},\hat{\mathbf{s}})}{\mathrm{d}s} = -\beta_\lambda I_\lambda(\mathbf{r},\hat{\mathbf{s}}) + \frac{\sigma_\lambda}{4\pi}\int_{4\pi} I_\lambda(\mathbf{r},\hat{\mathbf{s}}')\,p(\hat{\mathbf{s}},\hat{\mathbf{s}}')\,\mathrm{d}\Omega' \qquad (1)$$

Here I_λ represents the intensity ($\mathrm{W\,m^{-2}\,\mu m^{-1}\,sr^{-1}}$) of radiation of wavelength λ at point $\mathbf{r}$ in the medium, which travels a distance ds along the direction $\hat{\mathbf{s}}$. As expressed by the first term in the right-hand side of this equation, intensity is diminished due to both scattering and absorption. In particular, scattering takes some energy out from direction $\hat{\mathbf{s}}$ into all other directions. The attenuation is characterized by the extinction coefficient of the medium β_λ ($\mathrm{m^{-1}}$), which is the sum of the scattering σ_λ and absorption κ_λ coefficients. Nevertheless, there is also an increase of intensity due to scattering of radiation from other directions into the direction of interest $\hat{\mathbf{s}}$. This is accounted by the last term in the right-hand side of Eq. (1). The probability of scattering between two given directions $\hat{\mathbf{s}}$ and $\hat{\mathbf{s}}'$ is given by the phase function $p(\hat{\mathbf{s}},\hat{\mathbf{s}}')$. This function, and the coefficients σ_λ and κ_λ are determined by the kind of scattering particles present in the medium. The last two parameters also depend on particle concentration. Usually $\beta_\lambda = c_\mathrm{p}\beta^*_\lambda$ and $\kappa_\lambda = c_\mathrm{p}\kappa^*_\lambda$, where c_p is the concentration of catalyst particles, and β^*_λ, κ^*_λ are independent of this concentration. These two parameters have been measured for several commercial brands of TiO_2 [7,19]. The first expresses the ability of catalyst particles to absorb and scatter radiation; it is equal to the effective area projected by a unit mass of the particles to a radiation beam falling onto them. The second parameter accounts for absorption in an analogous manner.

Eq. (1) is an integro-differential equation in five variables (three spatial coordinates, and two angles for the propagation direction), and its analytical solution can be accomplished only in very restricted situations. As mentioned above, it is usually solved by numerical methods. However, due to the complications in the implementation of these methods and the large amount of computer calculations required, it is highly desirable to have approximate methods to solve the RTE. The P1 approximation is based on the assumption that the radiation field in any point inside the reactor comes from all directions with an almost isotropic distribution. Of course, if the radiation entering an scattering medium is very directional, a large amount of scattering is necessary to render it isotropic. Mathematically the assumption maybe stated as

$$I(\mathbf{r},\hat{\mathbf{s}}) = \frac{1}{4\pi}[G(\mathbf{r}) + \hat{\mathbf{s}}\cdot\mathbf{q}(\mathbf{r})] \qquad (2)$$

This expression involves the incident radiation

$$G(\mathbf{r}) = \int_{4\pi} I(\mathbf{r},\hat{\mathbf{s}}')\,\mathrm{d}\Omega' \qquad (3)$$

and the radiative flux vector

$$\mathbf{q}(\mathbf{r}) = \int_{4\pi} I(\mathbf{r}, \hat{\mathbf{s}}')\hat{\mathbf{s}}' \, \mathrm{d}\Omega' \tag{4}$$

The first term in the right-hand side of Eq. (2) is the intensity at point **r**, averaged over all directions. Actually, the amount of energy absorbed by unit volume in any point inside the medium is given by the product $\kappa_\lambda G(\mathbf{r})$. The second term of Eq. (2) gives the net flux of radiative energy traveling into direction $\hat{\mathbf{s}}$. In fact, **q** is the first moment of the intensity distribution with respect to angular coordinates. Thus, the P1 approximation is a first-order expansion for the intensity distribution in terms of the direction vector. Of course, for this expansion to be valid, the second term should be much smaller than the first.

Introducing the approximate form (2) for the intensity into the RTE (1), and after some lengthy manipulation, a second degree differential equation is obtained [11,12]

$$\nabla^2 G(\mathbf{r}) = K_\mathrm{d}^2 G(\mathbf{r}) \tag{5}$$

where

$$K_\mathrm{d} = \sqrt{3\kappa_\lambda \beta_\lambda (1 - \omega g)} \tag{6}$$

The transport constant K_d is sometimes called diffusion constant, for time dependent versions of Eq. (5) [11, Chapter 9]. The scattering albedo is defined as

$$\omega = \frac{\sigma_\lambda}{\beta_\lambda} \tag{7}$$

In this equation it also appears the asymmetry parameter, which characterizes the shape of the phase function,

$$g = \frac{1}{4\pi} \int_{4\pi} p(\hat{\mathbf{s}}, \hat{\mathbf{s}}')\hat{\mathbf{s}} \cdot \hat{\mathbf{s}}' \, \mathrm{d}\Omega' \tag{8}$$

The values of this parameter are between −1 and 1. In particular, for isotropic scattering it equals 0, while a value of 1 means that all radiation is scattered in the forward direction.

To solve for the incident radiation $G(\mathbf{r})$ it is necessary to have boundary conditions which can be used together with Eq. (5). For semitransparent boundaries the following condition is obtained [20]

$$(1 - \rho)G(\mathbf{r}_\mathrm{b}) - \frac{2(1 + \rho)}{3\beta_\lambda (1 - \omega g)} \hat{\mathbf{n}}_\mathrm{b} \cdot \nabla G(\mathbf{r}_\mathrm{b}) = 4q_\mathrm{ent}(\mathbf{r}_\mathrm{b}) \tag{9}$$

where $\mathbf{r}_\mathrm{b}$ is any point on the boundary, $\hat{\mathbf{n}}_\mathrm{b}$ the unit vector normal to the boundary at that point, ρ the internal reflectance of the wall, and q_ent is the entering radiation flux.

We consider the simplest case for Eq. (5), i.e. when the entering flux is uniform over all points $\mathbf{r}_\mathrm{b}$ in any cross-section of the reactor wall, $q_\mathrm{ent}(\mathbf{r}_\mathrm{b}) = q_0$. In a cylindrical coordinate system (r, θ, z) whose z-axis coincides with the axis of the reactor tube, this assumption means that the incident radiation $G(\mathbf{r})$ is independent of the angle θ. Also, due to the construction of the solar reactors the intensity can be considered independent of z. Then, Eq. (5) is transformed into an ordinary differential equation in the radial coordinate

$$\frac{\mathrm{d}^2 G}{\mathrm{d}r^2} + \frac{1}{r}\frac{\mathrm{d}G}{\mathrm{d}r} - K_\mathrm{d}^2 G = 0 \tag{10}$$

Eq. (10) has as solutions the modified Bessel functions $I_0^\mathrm{B}(K_\mathrm{d} r)$ and $K_0^\mathrm{B}(K_\mathrm{d} r)$. However, the second of these functions diverges at the origin (the center of the reactor), which would give an infinite amount of energy at that point. Therefore, the solution is expressed in terms of I_0^B only

$$G(r) = D I_0^\mathrm{B}(K_\mathrm{d} r) q_\mathrm{ent} \tag{11}$$

Substitution of this solution in the boundary condition (9) gives

$$D = \frac{4}{(1 - \rho) I_0^\mathrm{B}(K_\mathrm{d} r_0) + (2K_\mathrm{d}/3\beta_\lambda(1-\omega g))(1+\rho) I_1^\mathrm{B}(K_\mathrm{d} r_0)} \tag{12}$$

where r_0 is the radius of the reactor tube and I_1^B is another Bessel function, which is the derivative of I_0^B. Both of these functions are tabulated in [21].

To obtain the total amount of absorbed power per unit wavelength it is necessary to integrate $\kappa_\lambda G(r)$ over the whole reactor volume

$$P_\mathrm{abs} = \int_{V_\mathrm{T}} \kappa_\lambda G \, \mathrm{d}V = 2\pi l \kappa_\lambda \int_0^{r_0} G r \, \mathrm{d}r \tag{13}$$

this integration can be carried out analytically, with the help of Eq. (10), which gives $Gr = K_\mathrm{d}^{-1}(\mathrm{d}/\mathrm{d}r)(r \, \mathrm{d}G/\mathrm{d}t)$, and taking into account that I_1^B is the derivative of I_0^B. The final result is given by

$$P_\mathrm{abs} = \frac{2\pi l r_0 \kappa_\lambda D I_1^\mathrm{B}(K_\mathrm{d} r_0)}{K_\mathrm{d}} \tag{14}$$

where l is the length of the reactor tube. On the other hand, the total entering power per unit wavelength is

$$P_{\text{ent}} = 2\pi l r_0 q_{\text{ent}} \tag{15}$$

Dividing Eq. (14) by Eq. (15), the fraction of absorbed energy is obtained as

$$F_{1\lambda} = \frac{4\kappa_\lambda}{K_\text{d}} I_1^\text{B}(K_\text{d} r_0) \left[(1-\rho) I_0^\text{B}(K_\text{d} r_0) + (1+\rho) \frac{2K_\text{d}}{3\beta_\lambda(1-\omega g)} I_1^\text{B}(K_\text{d} r_0) \right]^{-1} \tag{16}$$

This expression turns out to be quite manageable if we realize that it takes into account multiple scattering in all directions, which is a very important issue in photocatalytic calculations [17]. The associated Bessel functions I_0^B and I_1^B are tabulated in standard reference books, and can also be evaluated with high accuracy from polynomial approximations [21]. An analytical formula can be obtained if we are interested in the maximum amount of energy that the reactor can absorb, which is achieved for large catalyst loads. In this case one has $K_\text{d} r_0 \gg 1$, and $I_0^\text{B} \approx I_1^\text{B} \approx \exp(K_\text{d} r_0)/\sqrt{2\pi K_\text{d} r_0}$ [21]. Then it is obtained that

$$F_{1\lambda}^{\max} = \frac{12\kappa_\lambda \beta_\lambda (1-\omega g)}{3(1-\rho)K_\text{d}\beta_\lambda(1-\omega g) + 2(1+\rho)K_\text{d}^2} \tag{17}$$

The model presented in this section will be compared in Section 6 with results from the MC method and from a very simple approximation of the LB type [18]

$$F_{1\lambda}^{\text{LB}} = 1 - \exp(-2\kappa_\lambda r_0) \tag{18}$$

3. MC method

The MC method is one of the numerical techniques used to obtain solutions to radiative transfer problems [9,10]. It is based on modeling radiation transport as a series of random events, where each photon is reflected, scattered, absorbed, etc. Here we briefly discuss the method used in this work. More comprehensive discussions of the MC method as applied to radiative transfer can be found elsewhere [12, Chapter 19].

The simulation procedure is as follows: photons are emitted one at a time, from the reactor wall into the scattering medium (suspension). The point of emission is selected randomly according to the flux distribution created in the wall by the solar concentrator under consideration. In the case of our PC we use distributions determined experimentally [22], in order to have a numerical solution which represents as close as possible the behavior of the reactor. The trajectory of each photon is tracked until it becomes absorbed or gets out of the reactor. A statistics of the outcome of the propagation of all these photons is kept, which allows to evaluate the fraction of radiation absorbed by the reactor.

Every time a photon reaches the reactor wall, its reflection or transmission is decided according to the outcome of a random number between 0 and 1. The reflectivity of the wall is interpreted as a probability for photon reflection. If the random number is smaller than this value the photon is reflected, otherwise it is transmitted and gets out of the reactor. After reflection or emission, the distance s to next encounter with the reactor wall is determined. Then, it is decided if the photon actually reaches the wall again or collides with a particle at some point in the trajectory. The probability of occurrence of such a collision is

$$p_{\text{ext}} = 1 - \exp(-\beta_\lambda s) \tag{19}$$

This probability is used to decide, according to a random number, which of the two possible events occurs. If the photon reaches the wall, the above procedure is repeated. On the other hand, if it is determined that the photon collides with a particle, the distance to the collision point is determined according to the probability density

$$f(x) = -\beta_\lambda \exp(-\beta_\lambda x) \tag{20}$$

As a result of a collision, a photon maybe either absorbed or scattered. The probability for the second event is given by the scattering albedo ω. This probability is used to determine the outcome of the collision. If scattering occurs, it is necessary to choose a new direction to propagate the photon from the collision point. This is done generating random numbers distributed according to the scattering phase function. Instead, if the outcome is absorption, the photon is accumulated to the count of absorbed photons and the process continues with the next photon.

A large number of photons is used, typically of the order 10^6, to obtain an accurate solution of the problem. At the end the fraction of absorbed radiation is determined as the quotient between the total number of

absorbed photons and the number of photons launched to the medium.

4. Experimental

Experiments were carried out in a PC able to concentrate radiation to 15 suns, which is shown schematically in Fig. 1. This collector tracks the sun about a north–south axis whose slope can be adjusted for each experiment to ensure normal incidence of beam solar radiation on its aperture. The collection surface is 1.82 m^2. The system has a tubular pyrex glass reactor with an inner diameter of 2.22 cm. The total system volume is 2.67 l, including piping and reactor. This device has been used previously for the degradation of sodium dodecylbenzensulfonate (DBSNa) [23,24].

The TiO_2 (>99% anatase) used as catalyst was obtained from Aldrich as reactive grade product. Carbaryl was used in a commercial pesticide formulation known as Sevin (80% active ingredient). Several TiO_2 concentrations were tested in order to determine its influence on the degradation. Catalyst and initial carbaryl concentrations are shown in Table 1, which also presents the total run time for each experiment and the conversion obtained. The suspension was circulated in the system under aerobic conditions and illuminated for a specific period using solar irradiation. Samples from the degradation runs were filtered using a 0.45 μm millipore filter membrane to separate the catalyst and were analyzed for carbaryl concentration by UV spectroscopy at 288 nm.

Table 1
Experimental parameters for the photocatalytic degradation of carbaryl in the solar collector

c_p (g/l)[a]	c_0 (mg/l)[b]	T (h)[c]	x (%)[d]
0.01	63.2	2	15.1
0.05	59.8	2	59.7
0.2	67.2	2	23.0
0.7	64.1	2	47.8
1.4	51.4	5.5	88.8
2.8	46.7	5.5	88.9

[a] Catalyst concentration.
[b] Initial carbaryl concentration.
[c] Total run time for the experiment.
[d] Total conversion.

The PC utilizes direct normal solar UV radiation. The amount of this radiation was determined

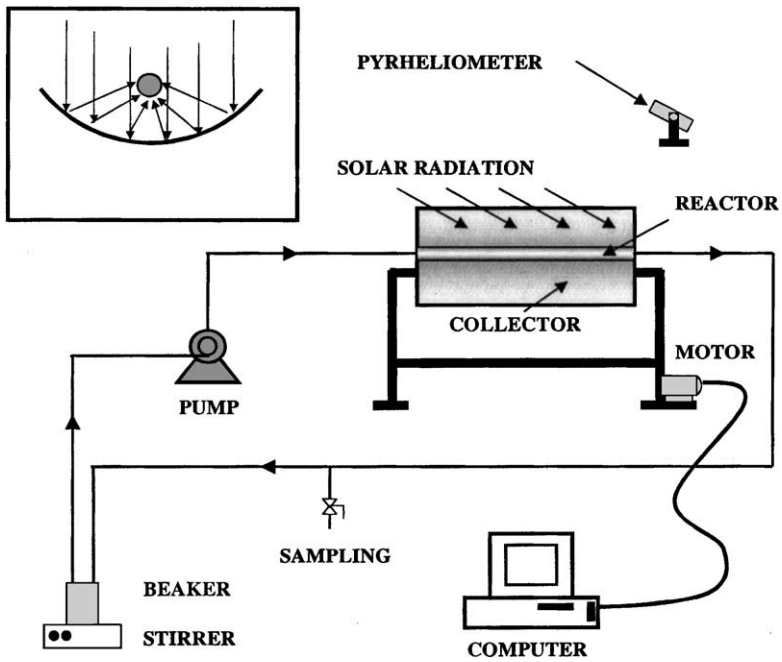

Fig. 1. Experimental setup. Inset: cross-section of the PC.

using suitably corrected measurements from an Eppley pyrheliometer with a Schott UV long-pass filter GG395.

5. Calculation of kinetic constants

We will assume that the local reaction velocity depends with a power law on radiation intensity [25–27], and that first-order kinetics exists. This is expressed by the following equation:

$$\frac{\mathrm{d}c_{\mathrm{L}}(\mathbf{r})}{\mathrm{d}t} = -k[e_{\mathrm{L}}(\mathbf{r})]^{\alpha} c_{\mathrm{L}}(\mathbf{r}) + R_{\mathrm{m}} \tag{21}$$

where $c_{\mathrm{L}}(\mathbf{r})$ is the local reactant concentration at point $\mathbf{r}$ of the system. The term R_{m} is the variation of this concentration due to mass transfer processes. The rate constant k depends on the kinetic and equilibrium constants for the reactions occurring in the system, on the quantum yield for the generation of charge carriers in the catalyst, and on the exponent α. This exponent takes values between 0.5 and 1 for kinetically limited reactions [25–27]. The quantity $e_{\mathrm{L}}(\mathbf{r})$ is the local volumetric rate of energy absorption (LVREA; the radiative energy absorbed in a given location of the reactor by unit time and unit volume), which varies from point to point within the reactor. The LVREA should be expressed in units of einstein (number of photons divided by Avogadro's number) per unit time and volume. The next step is to integrate Eq. (21) over the total system volume V_{T} and divide it by the same volume, to obtain the variation of the average reactant concentration c with time. If the system operates without mass transfer limitations (i.e. under a perfect mixing regime) the integration can be performed easily giving

$$\frac{\mathrm{d}c}{\mathrm{d}t} = -c\frac{k}{V_{\mathrm{T}}}\int_{V_{\mathrm{R}}} [e_{\mathrm{L}}(\mathbf{r})]^{\alpha}\,\mathrm{d}V \tag{22}$$

In this expression V_{R} is the volume of the reactor, which is the only part of the system where the LVREA is different from zero. All of the above assumptions are intended to simplify the analysis. Latter we will see that this model allows us to reproduce correctly the trends observed in our experiments.

The LVREA at any point inside the reactor is related to $G(r)$ by the equation

$$e_{\mathrm{L}}(r) = \frac{1}{N_{\mathrm{a}}hc_{\mathrm{light}}}\int_{300}^{400} \lambda\kappa_{\lambda} G(r)\,\mathrm{d}\lambda \tag{23}$$

where N_{a} is Avogadro's number, h the Planck's constant, and c_{light} is the speed of light. To determine the local radiation with Eq. (11) we need to know the entering radiation flux q_{ent} for each wavelength. This flux can be expressed in terms of the parameters of the solar collector and the arriving UV radiation $W(t)$ ($\mathrm{W\,m^{-2}}$), as measured by a radiometer, by the expression

$$q_{\mathrm{ent}} = W(t) f_{\lambda} C_{\mathrm{g}} \tau_{\lambda} \eta_{\mathrm{eff}} \tag{24}$$

The factor f_{λ} is the spectral distribution of solar radiation normalized to unity in the UV wavelength interval, from 300 to 400 nm. This factor is intended to separate the total UV radiation measurement into its components for different wavelengths, as required for the calculations with Eq. (23). Due to the position of the sun during the experiments, it is appropriate to use a standard AM1.5 solar spectrum for f_{λ} [28]. The other parameters in Eq. (24) are properties of the solar collector: the geometrical concentration C_{g}, the transmittance of the glass tube τ_{λ} and the optical efficiency factor η_{eff}. This factor expresses the ability of the concentrator to place the collected energy in the reactor, and is equal to the fraction of radiation entering the reactor with respect to the maximum possible. The procedure to determine this factor, based on the actinometric reaction between the oxalic acid and uranile salt, has been described previously by Curcó et al. [3]. Following this procedure, we have determined an efficiency of $\eta_{\mathrm{eff}} = 0.69$ for our PC.

Substituting Eqs. (11), (23) and (24) into Eq. (22) we get

$$\frac{\mathrm{d}c}{\mathrm{d}t} = -c\frac{k}{V_{\mathrm{T}}}\int_{V_{\mathrm{R}}} \left\{ \frac{1}{N_{\mathrm{a}}hc_{\mathrm{light}}}\int_{300}^{400} \lambda\kappa_{\lambda} D I_0^{\mathrm{B}}(K_{\mathrm{d}}r) W(t) \times f_{\lambda} C_{\mathrm{g}} \tau_{\lambda} \eta_{\mathrm{eff}}\,\mathrm{d}\lambda \right\}^{\alpha} \mathrm{d}V \tag{25}$$

Integrating Eq. (25) with respect to time we arrive to an expression for the reactant concentration as a function of time

$$\ln\left[\frac{c(t)}{c_0}\right] = -B_{\alpha}(c_{\mathrm{p}})\int_0^t [W(t')]^{\alpha}[V_{\mathrm{T}}(t')]^{-1}\,\mathrm{d}t' \tag{26}$$

where

$$B_{\alpha}(c_{\mathrm{p}}) = 2\pi lk\left[\frac{C_{\mathrm{g}}\eta_{\mathrm{eff}}}{N_{\mathrm{a}}hc_{\mathrm{light}}}\right]^{\alpha}\int_0^{r_0} r\,\mathrm{d}r \times \int_{300}^{400} [\lambda f_{\lambda}\tau_{\lambda}\kappa_{\lambda} D I_0^{\mathrm{B}}(K_{\mathrm{d}}r)]^{\alpha}\,\mathrm{d}\lambda \tag{27}$$

In this expressions c_0 is the initial reactant concentration and l is the length of the reactor tube. Note that the system volume reduces with time due to the sampling carried out during the experiment. Thus, it cannot be taken out of the integral of Eq. (26). That equation expresses the evolution of the logarithm of concentration as the time integral of the αth power of the incoming radiation. Within this theoretical model, the proportionality factor B_α depends only on the catalyst concentration trough the LVREA.

From the experimental data, and assuming a given value for the exponent α, the left-hand side and the integral on the right-hand side of Eq. (26) can be evaluated. Then B_α is obtained as the quotient of both quantities. On the other hand, this parameter can also be evaluated theoretically from Eq. (27) by carrying out the integrals numerically. In the next section, the values calculated from the experimental data with the first method are fitted with the theoretical values obtained from Eq. (27), to obtain the parameters k and α of the process.

6. Results and discussion

First we present the results of calculations of radiation absorption in the tubular reactor with a suspension of TiO_2 catalyst particles. For all the calculations we use the absorption and scattering cross-sections for the Aldrich catalyst reported in [7]. Also we assume an isotropic phase function as recommended in [19]. In particular, we compare the P1 and LB (Eq. (18)) approximations against the results of MC simulations. Later, the absorption results are used to evaluate the rate constants for carbaryl degradation in the PC.

In Fig. 2 we present the results for the fraction of absorbed radiation $F_{1\lambda}$ as a function of wavelength, calculated for different catalyst concentrations. In general, a good correspondence between the P1 approximation and the numerical results from the MC method is observed. Actually, the overall error introduced by the approximation is never larger than 12%. This error is mainly due to the fact that the radiation flux entering the reactor tube is quite directional. Actually, the

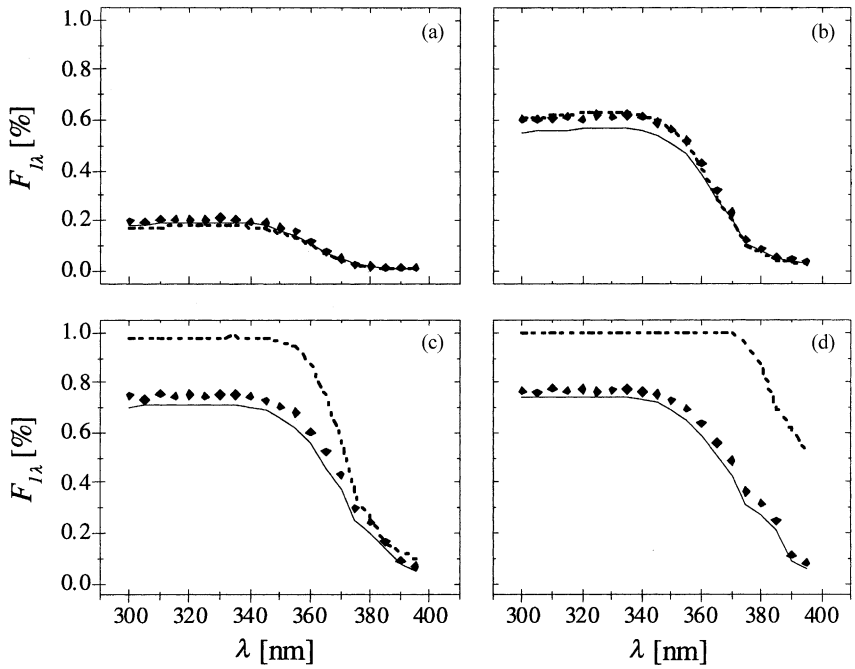

Fig. 2. Fraction of absorbed radiation calculated with three methods: P1 approximation (solid line), MC simulations (points) and LB approximation (dashed line). The catalyst concentrations considered are (a) 0.01 g/l, (b) 0.05 g/l, (c) 0.2 g/l, and (d) 0.7 g/l.

deviation of the surface of our parabolic concentrator from specular reflection has been determined to be 0.4° [22]. Taking into account the diameter of the reactor and the dimensions of the concentrator, the angles of incidence of light in the reactor can be calculated. It turns out that these incidence angles are at most 31° with respect to the normal of the outer glass surface. Moreover, due to the refraction of light when it passes from air to water through the glass wall, the maximum angle is reduced to 23°. The above means that the P1 approximation assumption of almost isotropic intensity is not fulfilled close to the wall. The consequence of this is larger paths for photons through the medium on the average, and therefore more absorption. This explains the larger fraction of absorbed radiation predicted by the MC simulations as compared to the P1 approximation. Moreover, this points out to the possibility of future improvement of the model by exploring alternative definitions for the K_d [20]. Also, it must be pointed out that in the MC simulations we are using a measured flux distribution outside the reactor, while in the P1 approximation we consider this distribution as homogeneous in order to have mathematical simplification. This is another source of error.

The LB approximation shows reasonable agreement with the MC results only for small catalyst concentrations (Fig. 2a and b). This is to be expected because these kind of approximations are not able to deal properly with scattering. Indeed, the LB calculation predicts an almost complete absorption for the short wavelengths in the case of $c_p = 0.7$ g/l. On the other hand, the P1 approximation results display the correct saturation behavior for large concentrations of particles (Fig. 2c and d). The saturated value is given by the asymptotic result of Eq. (17). Physically the reason for the saturation of absorption is the backscattering of radiation by the catalyst particles. The result of this effect is that a fraction of radiation is effectively redirected towards the glass wall and escapes from the reactor, which prevents complete absorption of the entering radiation [17].

With the above results in mind, we will use the P1 approximation, which requires much less numerical calculations than the MC method, for all the subsequent calculations. In Fig. 3 the radial distribution of absorbed radiation, is presented. This quantity is equal to the local radiation, multiplied by r and κ_λ, and divided by the entering flux. Such a product yields a dimensionless quantity, which is directly proportional to the radiation absorbed by unit radius and unit reactor length. This distribution must be regarded as an average of the radial distributions for different values of θ, since we have assumed that the incident flux was the same all over the reactor wall in order to reduce the complexity of the model. It is clearly seen how for small catalyst loads the radiation is absorbed in a more uniform way in the whole reactor. As the concentration of particles increases the absorption gradually shifts towards the wall, leaving large portions of the center of the reactor completely shaded. As pointed out by several authors [4,6,9,29], this shading may reduce the efficiency of the degradation process.

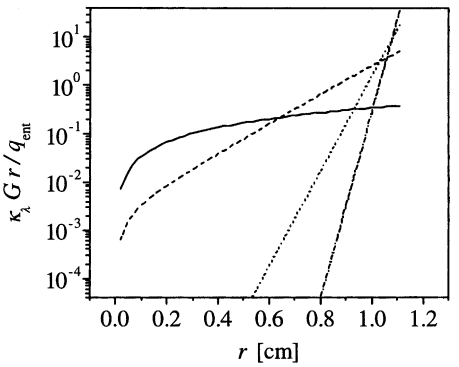

Fig. 3. Radial distribution of absorbed radiation, as a function of the radial coordinate, according to the P1 approximation. Specifically, the local radiation multiplied by the radius and divided by the entering flux is presented. Four different catalyst concentrations are considered: 0.01 g/l (solid line), 0.2 g/l (dashed line), 0.7 g/l (dotted line), and 1.5 g/l (dash-dotted line).

The proportionality factor B_α, as calculated theoretically from Eq. (29), is presented in Fig. 4. The values for the parameter k have been arbitrarily adjusted to allow direct comparison of the behavior for different values of the exponent α. Quite different trends are obtained depending on that value. All the curves have an inflection point around a concentration of 0.2 g/l. For exponents larger than approximately 0.85 the factor is seen to increase monotonically with the catalyst concentration, with two clearly different regions to each side of the inflection point. On the other hand, for values of α smaller than 0.85 the curves have a maximum on this point, after which the factor decreases with concentration. The case with exponent 0.85 varies relatively little after 0.2 g/l. This

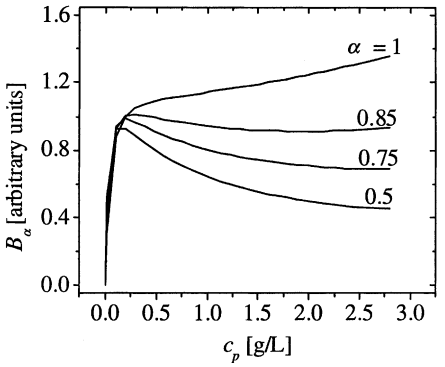

Fig. 4. Proportionality constant for the degradation of carbaryl, as a function of the catalyst load, calculated from the theoretical model for different values of α. The height of the curves is adjusted arbitrarily to plot them together.

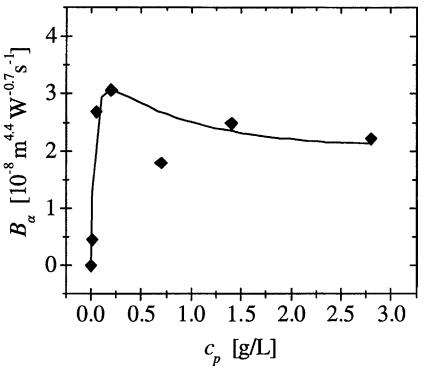

Fig. 5. Proportionality constant for the degradation of carbaryl, as a function of the catalyst load. The results are calculated from the experimental data (points), and fitted using the theoretical model (line).

particular value of concentration corresponds with the beginning of important saturation of the absorption in the reactor, as seen from Fig. 2.

The decreasing behavior for large catalyst loads, in the case of the smaller values of the exponents, expresses the decrease of the effectiveness of the reactor due to the shading of its center at high catalyst loads. For $\alpha = 1$ this behavior is not observed. This is so because in this case the B_α factor is proportional to the volumetric integral of the local radiation, i.e. it is proportional to the total radiation absorbed by the reactor. This quantity does not decrease with increasing absorption, but saturates as discussed previously. There are, however, two different regions on the curve of $\alpha = 1$. The first finishes with the onset of strong saturation for short wavelengths at $c_\mathrm{p} = 0.2$ g/l. However, for this value of concentration the absorption for the large wavelengths is not fully saturated yet (Fig. 2; above 360 nm). The slower increase of the second portion of the curve is related to the slower saturation of this long wavelength absorption. It must be taken into account that the solar UV spectrum has a higher fraction of radiation with longer wavelengths. Then, the contribution of this part of the spectrum to the integral in Eq. (27) is higher than it may appear from Fig. 2.

As explained in section 5, the determination of k and α is done by fitting the experimental values of B_α, calculated with Eq. (26), by those calculated theoretically with Eq. (27). The two unknown quantities are used as fitting parameters in this procedure, and the results are presented in Fig. 5. In particular, the present fit is obtained with $\alpha = 0.72$ and $k = 2.2 \times 10^{-3}(\mathrm{einstein\,m^{-3}})^{-0.72}\,\mathrm{s}^{-0.28}$. As can be seen, the theoretical model very well reproduces the observed experimental trends. It is interesting to notice that the peak in the curve seems to be close to the experimental results. Also, the position of this peak lies in the range reported in the literature for other substances [23,29]. In the theoretical model the location of the peak depends mainly on the values of the scattering and absorption coefficients of the catalyst particles, and on the tube radius. In particular, we have taken the values reported by Brandi et al. [7] for the Aldrich catalyst. We, would like to point out that the fit we have obtained is not very conclusive, because it its done with few experimental points. However, the kinetic model and the radiation absorption model seem to reproduce the experimental trends well.

7. Conclusions

We have presented an analytical model to evaluate the absorbed radiation in a tubular photocatalytic reactor. This model is based on the P1 approximation to the RTE. It is able to account for radiation scattering in all directions and does not contain adjustable parameters. The model has been compared to the results of MC simulations and to an approximation of the LB type. It is found that the model has the same qualitative behavior than the simulations,

with an error not larger than 12%. This error is attributable to the inability of the model to deal with the very directional behavior of radiation intensity near the reactor wall. The P1 approximation displays the correct saturation behavior for absorption at large concentrations, in contrast with the LB approximation that predicts full absorption of the entering radiation flux.

We carried out experiments for the degradation of carbaryl in a parabolic trough collector, for different catalyst concentrations. The kinetic model used gives quite different behaviors for the degradation rate as a function of catalyst load, depending on the value chosen for α. The calculations from the theoretical model have been fitted to the experimental results, in order to obtain the rate constant and the exponent for the degradation process. The values obtained are $\alpha = 0.72$ and $k = 2.2 \times 10^{-3}(\text{einstein m}^{-3})^{-0.72}\,\text{s}^{-0.28}$. The more efficient degradation seems to be reached with catalyst concentrations around 0.2 g/l. The radiation absorption and kinetic model reproduce well the main features observed in the experiment.

Acknowledgements

This work was founded by Consejo Nacional de Ciencia y Tecnología, Mexico (grants 37636-U and J36640-E). The authors thank J.J. Quiñones Aguilar for technical assistance.

References

[1] O.M. Alfano, D. Bahnemann, A.E. Cassano, R. Dillert, R. Goslich, Catal. Today 58 (2000) 199.
[2] M. Romero, J. Blanco, B. Sánchez, A. Vidal, S. Malato, A.I. Cardona, E. García, Sol. Energy 66 (1999) 169.
[3] D. Curcó, S. Malato, J. Blanco, J. Jiménez, P. Marco, Sol. Energy 56 (1996) 387.
[4] A.E. Cassano, O.M. Alfano, Catal. Today 58 (2000) 167.
[5] C.A. Martín, G. Sgalari, F. Santarelli, Ind. Eng. Chem. Res. 38 (1999) 2940.
[6] C.A. Martín, G. Camera-Roda, F. Santarelli, Catal. Today 48 (1999) 307.
[7] R.J. Brandi, O.M. Alfano, A.E. Cassano, Chem. Eng. Sci. 54 (1999) 2817.
[8] R.L. Romero, O.M. Alfano, A.E. Cassano, Ind. Eng. Chem. Res. 36 (1997) 3094.
[9] M. Pasquali, F. Santarelli, J.F. Porter, P.-L. Yue, AIChE J. 42 (1996) 532.
[10] C.A. Arancibia-Bulnes, J.C. Ruiz-Suárez, Appl. Opt. 38 (1999) 1877.
[11] A. Ishimaru, Wave Propagation and Scattering in Random Media, Oxford University Press, Oxford, 1997.
[12] M.F. Modest, Radiative Heat Transfer, McGraw-Hill, New York, 1993.
[13] K.M.S. Sundaram, S.Y. Szeto, J. Environ. Sci. Health B22 (1987) 579.
[14] M.M. Halmann, Photodegradation of Water Pollutants, CRC Press, New York, 1996, p. 301.
[15] Y. Sun, J.J. Pignatello, J. Agric. Food Chem. 41 (1993) 308.
[16] N. De Bertrand, D. Barceló, Anal. Chim. Acta. 254 (1991) 235.
[17] R.J. Brandi, O.M. Alfano, A.E. Cassano, Environ. Sci. Technol. 34 (2000) 2623.
[18] A. Brucato, L. Rizzuti, Ind. Eng. Chem. Res. 36 (1997) 4740.
[19] M.I. Cabrera, O.M. Alfano, A.E. Cassano, J. Phys. Chem. 100 (1996) 20043.
[20] T. Spott, L.O. Svaasand, Appl. Opt. 39 (2000) 6453.
[21] F.W.J. Olver, in: M. Abramowitz, I.A. Stegun (Eds.), Handbook of Mathematical Functions, Dover, New York, 1972, Chapter 9.
[22] J.C. Domínguez Alvarez, Tesis de Licenciatura, Facultad de Ingeniería y Ciencias Químicas, Universidad Autónoma del Estado de Morelos, Mexico, 1998 (in Spanish).
[23] A.E. Jiménez, C.A. Estrada, A.D. Cota, A. Román, Sol. Energy Mater. Sol. Cells 60 (2000) 85.
[24] S. Gelover, T. Leal, E.R. Bandala, A. Román, A. Jiménez, C.A. Estrada, Water Sci. Technol. 42 (2000) 101.
[25] C.S. Turchi, D.F. Ollis, J. Catal. 122 (1990) 178.
[26] D. Bahnemann, D. Bockelman, R. Goslich, Sol. Energy Mater. 24 (1991) 564.
[27] D.M. Blake, J. Webb, C. Turchi, K. Magrini, Sol. Energy Mater. 24 (1991) 584.
[28] R. Hulstrom, R. Bird, C. Riordan, Sol. Cells 15 (1985) 362.
[29] J. Giménez, D. Curcó, M.A. Queral, Catal. Today 54 (1999) 229.